Customer	**ESRIN**	**Document Ref**	**:**	**BAQ-TEC-TEN-SER-048**
Contract No	**4000126749/19/I-NS**	**Issue Date**	**:**	**17 December 2021**
WP No	**4100**	**Issue**	**:**	**1.0**

Reduction of NO2 amounts during the Italian lockdown period

Abstract This technical note describes the procedure used to investigate the reduction of NO2 amounts during the Italian lockdown period, using PGN, in situ and TROPOMI products

Author Gabriele Mevi
SERCO

Approval Anna Maria Iannarelli
on behalf of BAQUNIN Team

Distribution ESA/ESRIN EOP-GMQ
BAQUNIN Team

Serco Italia SpA
Sede Operativa: Via Sciadonna, 24-26 - Frascati (Roma)
Tel: +39 06 98354400 Fax:
www.serco.com

Change History

This document shall be amended by releasing a new edition of the document in its entirety. The Amendment Record Sheet below records the history and issue status of this document.

ISSUE	DATE	REASON
1.0	17 Oct 2021	First version

1- INTRODUCTION

Document Objective

This document describes the procedure used to investigate the reduction of NO2 amounts during the Italian lockdown period, using PGN, in situ and TROPOMI products. The dataset, the methodology and the analysis results are described in detail.

Document Scope

The analysis mainly focused on the exploitation of the datasets provided by the PGN Pandora instruments which are part of BAQUNIN instrumental suite: PAN#117 installed in the Rome city center (APL site) and in operation since May 2016 (replaced by PAN#138 between 2019 and 2020), and PAN#115 operating in the semi-rural surroundings of Rome (CNR-ISAC site) since March 2017. These long series of data are used to compare the amounts of atmospheric NO2 observed during the Italian lockdown period, to those acquired during so called "normal period", i.e., relative to the years 2017-2019.

In order to ensure the data homogeneity, a preliminary data screening has been performed based on available quality flags and uncertainty information. Then, the data relative to the period pre-lockdown are used to create NO2 look-up tables (LUTs), which provide "reference concentrations" to be compared with NO2 values retrieved during lockdown period. In this technical note, each phase of the procedure is described in detail as the results of the data analysis and the comparison with NO2 concentrations measured by in situ and TROPOMI instruments.

Finally, qualitative information about vehicular traffic variations is used to assess the validity of the analysis outcomes.

Document Structure

Chapter 1 (this one) contains an overview of the technical note objective and scope.

Chapter 2 contains a description of the italian government restriction actions to limit the COVID-19 pandemic spread and the effects on NO2 amount

Chapter 3 contains a detailed description of the Pandora NO2 dataset used in this study

Chapter 4 shows the results of the analysis of NO2 reduction during lockdown period and the comparison with NO2 measurements from in situ and satellite (TROPOMI) instruments

ACRONYMS

Acronym	Definition
APL	Atmospheric Physics Laboratory
ARPA	Regional Agency for Environmental Protection
ARSIAL	Regional Agency for the Development and Innovation of Agriculture of Lazio
ATBD	Algorithm Theoretical Baseline Document
BAQUNIN	Boundary-layer Air Quality-analysis Using Network of Instruments
CNR-IIA	National Research Council of Italy, Institute of Atmospheric Pollution Research
CNR-ISAC	National Research Council of Italy, Institute of Atmospheric Sciences and Climate
COR	Pearson correlation coefficient
DPCM	Decree of the President of the Council of Ministers (Decreto del Presidente del Consiglio dei Ministri)
DQF	Data Quality Flag
DU	Dobson Units
GU	Official Journal (Gazzetta Ufficiale)
IRDC	Interpolated Reference Daily Cycles
LUT	Look-Up Table
MAX-DOAS	Multi-Axis Differential Optical Absorption Spectroscopy
PGN	Pandonia Global Network
Ppb	parts per billion
RDC	Reference Daily Cycles
RMS	Root-Mean Square
SC	near-surface concentration
TC	Tropospheric Columns
UTC	Coordinated Universal Time
UV	Ultraviolet
VC	Vertical Column
VIS	Visible
WHO	World Health Organization

2- CONTEXT: ITALIAN GOVERNMENT RESTRICTIONS TO LIMIT THE PANDEMIC SPREAD

On January 7, 2019, the World Health Organization (WHO) announced the identification of a new virus, named SARS-CoV-2 (WHO, 2020). During the following weeks, the virus spread around the globe, and, in March 2020, the epidemic turned into a pandemic that forced worldwide authorities to take increasingly severe measures to limit the spread of the virus.

In February 2020, COVID-19 virus outbreak begins in Italy, forcing the Italian government to adopt unprecedented actions to face the pandemic. A Decree of the President of the Council of Ministers (Decreto del Presidente del Consiglio dei Ministri, hereinafter, DPCM) published in the Official Journal (Gazzetta Ufficiale, GU) decreed a lockdown state for all the country with the temporary closure of the major part of production, public and commercial activities, and severe restrictions to public and private mobility. On February 23, 2020, some areas in Northern Italy were locked (GU n. 45, hereinafter, DPCM-1) and severe restriction measures were adopted in the whole country. The Italian lockdown started officially on March 9, 2020, when the DPCM-2 was published (GU n. 59). Other relevant DPCMs in this context are the DPCM-3 (22 March, GU n. 76) that suspends non-essential activities, DPCM-4 (27 April, GU n. 108) that allowed the reopening of selected activities and factories from the 4 May, and DPCM-5 (17 May, GU n. 126) that stated much less restrictive measures from 15 June. This latter date can be considered as the official end of the Italian lockdown.

The lockdown measures have affected most of the world, limiting industrial activities, travel, local and long-range transports. Due to these restrictions, significant improvements in air quality levels, especially for NO_2, have been confirmed in different regions of the planet. Most of the scientific works, however, focused on the analysis by means of satellite data, with temporal averages that do not allow us to consider the daily variations of NO_2 or the differentiation between working days and weekends. In particular, preliminary satellite-based studies indicate an important reduction in NO_2 levels in India (ESA, 2020), China (Liu et al., 2020), Spain (Mesas-Carrascosa, 2020), Brazil (Nakada, 2020), Iraq (Hashim, 2020) and USA (Goldberg, 2020), among others.

Several studies have shown a net decrease in the atmospheric content of NO_2 in Italy due to restrictions (Cameletti, 2020; Filippini et al., 2020, Campanelli et al., 2021). Bassani et al. (2020) compared tropospheric NO_2 vertical column density from the TROPOspheric Monitoring Instrument (TROPOMI) and in situ data, provided by ground-based air quality stations, in order to evaluate the spatial-temporal variations of the NO_2 in Rome and the surrounding rural areas. They found a sharp decline in NO_2 concentrations both in urban (-43% and -44%, TROPOMI and in-situ measurements, respectively) and rural (-17% and -20% TROPOMI and in-situ measurements, respectively) areas.

In this technical note, we analyze the NO_2 columnar (total and tropospheric) densities and near-surface concentrations collected by two Pandora 2S sun-spectrometers (Herman et al., 2009), belonging to the Pandonia Global Network (PGN, https://www.pandonia-global-network.org/) and part of BAQUNIN instrumental suite. The urban site is located in Rome at the Physics Department of Sapienza University under the responsibility of the Atmospheric Physics Laboratory (hereafter APL), the CNR-ISAC site is placed in the South-East area of Rome in a semi-rural environment. The coordinates and the elevation above sea level of the sites are reported in Table 1 as well as the identification numbers of the Pandoras.

Site name	Component	Latitude	Longitude	Elevation (m.a.s.l.)	PGN ID
APL	Urban	41.901	12.516	75	Pan#117 - Pan#138*
CNR-ISAC	Semi-Rural	41.840	12.647	117	Pan#115

* Pan#138 temporarily operated at APL from 28 August to 18 September 2019 and from 24 July and 11 September 2020.

Table 1: Details of the BAQUNIN observation sites.

3- DATASET

Pandora NO2 measurements

The PGN Pandora 2S sun-spectrometers perform measurements of direct and diffuse solar radiation in the spectral range 290-900 nm using two spectrometers (UV spectrometer: 290 to 530 nm, with a resolution of 0.6 nm; VIS spectrometer: 380 to 900 nm, with a resolution of 1.1 nm) to estimate total column, tropospheric column, and surface concentration of several gases. The PGN retrieval schemes for NO2 and other trace gases from direct sun measurements, including the so-called Algorithm Theoretical Baseline Document (ATBD) and the guidelines for the correct use of PGN products are detailed in Cede (2019) and Cede et al. (2019). The radiance spectra underpass several correction/adjustment procedures, such as dark signal, non-linearity, latency, flat field, temperature, stray light, sensitivity, and wavelength corrections (details in Cede, 2019), before the retrieval of geophysical quantities.

The NO2 vertical total column density (hereinafter, VC) is defined as the NO2 total column amount between the altitude of the instrument and the top of the atmosphere. VCs are measured in direct Sun observation mode, in which the sampled air mass is a circular cone with its apex at the entrance of the instrument and extending into the direction of the Sun. This means that, for Northern Hemispheric locations, the measurements sample air towards East in the morning, South around noon, and West in the afternoon.

The PGN instruments can operate in the Multi-Axis Differential Optical Absorption Spectroscopy (MAX-DOAS) measurements mode. It consists of spectral measurements of scattered sunlight under different viewing elevation angles, and it is suitable for the determination of trace gases columns within the lower troposphere (Hönninger et al., 2004). The MAX-DOAS algorithm exploits measurements from five pointing zenith angles (0, 60, 75, 88, 89 degrees) at a fixed azimuth direction. Since the algorithm is fully parameterized, no elaborate radiative transfer calculations are needed and, hence, real time data delivery is still given. Currently near-surface concentration (SC) and tropospheric columns (TC) of NO2 are extracted from this algorithm. Details about the retrieval schemes can be found in Cede (2019) and in Spinei et al. (2020). The NO2 VCs and TCs (column amount) are expressed in Dobson Units (DU, with 1 DU=2.687×10^{20} molecules per square meter), while NO2 SCs are given in parts per billion (ppb). All data used in the present study are screened by considering only high and medium data quality (i.e., with Data Quality Flag (DQF) – in the PGN files equal to 0, 1, 10 and 11). The precision of the NO2 column amounts for DQF=0 is <0.005 DU, the accuracy is estimated to 0.05 DU at the one standard deviation level (Herman et al., 2009).

Note that the operating efficiency of the Pan#115 has been degrading over time, leading to the refurbishment of the instrument in November 2020. For this reason, in what follows, the results from July 2020 of Pan#115 must be taken with a degree of caution but they have been considered anyway to allow a rough comparison with the other instruments and variables.

Reference dataset

CNR-ISAC dataset analyzed in this paper is composed by Pan#115 measurements acquired from March 2017 to November 2020, when the operating efficiency of the instrument significantly degraded (sun tracker issues), leading to the necessity to stop operations for full refurbishment of the instrument. For this reason, in what follows, the results from July 2020 of Pan#115 must be taken with a degree of caution.

APL dataset is composed merging the Pan#117 time series (from May 2016 to September 2019 and from 11 September 2020 to date) with that of Pan#138 (from September 2019 to 11 September 2020). In order to inter-calibrate the instruments and create a robust APL dataset with a verified self-consistency, two testing phases in which Pan#117 and Pan#138 were installed in the same site have been designed. Pan#117 and Pan#138 operated together at APL from 28 August to 18 September 2019 and from 24 July and 11 September 2020.

Figure 1 shows the scatter plots between Pan#138 (y-axis) and Pan#117 (x-axis) NO_2 VC data collected in the inter-calibration period of 2019 (panel a) and 2020 (panel b). As can be depicted from the results, the retrievals from the two instruments are self-consistent, with excellent correlation (>0.99), negligible bias (<0.02) and very small RMS

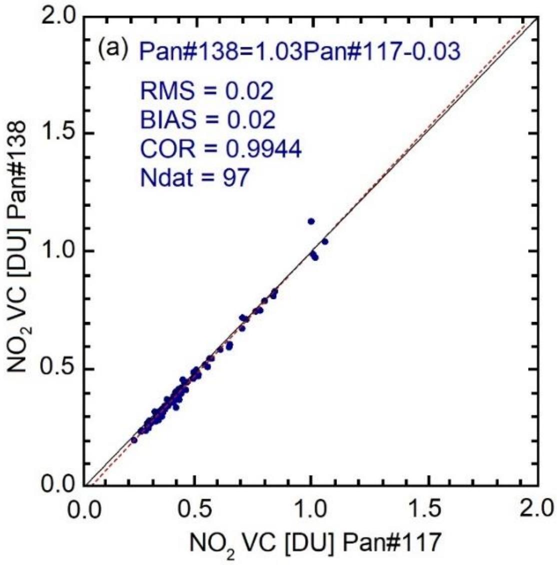

(0.02).

Figure 1: Pan#138 vs. Pan#117 NO_2 VCs scatter plots for 28 August – 18 September 2019 (a) and 24 July – 11 September 2020 (b). The reported statistical parameters are root-mean square of differences (RMS) [DU], mean bias (BIAS) [DU], linear Pearson correlation coefficient (COR) and number of valid retrievals (Ndat). Dashed lines indicate the linear fit between the two instruments, while solid lines indicate the ideal fit $x = y$.

In order to assess the impact of lockdown and restriction measurements on retrieved NO_2 concentrations, a reference is needed for comparison. Ideally, a thirty-year time series should be used to construct a climatological reference (WMO, 2017); by excluding 2020 only few full years of data are available to build-up “climate normal”.

Despite the non-negligible impact of meteorological variability on the interpretation of the results, the comparison between the reference climatological series and the observations collected during the lockdown highlighted interesting features, albeit the comparatively limited period covered. In particular, the differences between the urban and semi-rural environments appear to be well captured, as well as seasonal, daily and hourly variations.

The NO_2 APL and CNR-ISAC time series have been used to create a reference climatological dataset of VC, TC and SC for both the BAQUNIN sites, depicted hereinafter in the so-called reference “look-up table” (LUT).

Firstly, the data were classified as “workdays”, i.e. collected from Monday to Friday, and “weekends”, i.e. collected on Saturdays and Sundays. The PGN NO_2 products were further screened by requiring the retrieval (fitting) percentage uncertainty smaller than

10% for VCs and of 40% for both TCs and SCs. Moreover, data retrieved with solar zenith angle greater than 80 degrees were excluded. Secondly, for each month of the year, the valid NO_2 data were grouped according to their measurement fractional hour in steps on 1 hour between 00:00 and 24:00 UTC. Finally, for each hourly bin, the data average, standard deviation, median and number of samples were retrieved.

This procedure allows for the creation of NO_2 VC, TC and SC reference LUTs, function of the month of the year and of the hour of the day. Each variable is associated to two different LUTs: the former is obtained using workday's data, the latter considering only weekend's data. The aim of this division is to take into account the differences in the NO_2 daily cycle produced by the traffic reduction during weekends.

Figures 2 and 3 show the reference NO_2 VC, TC and SC LUTs for APL (left column) and CNR-ISAC (right column) for workdays and weekends, respectively. As expected, the APL (urban) NO_2 values are higher than that of CNR-ISAC (semi-rural). The most relevant feature of the LUTs is the evident seasonal variation of the NO_2 peak value correlated to the Sun illumination over the year for both the urban and semi-rural sites. In fact, the VC and TC peak values are observed at about 14:00 UTC between November and January while, for June and July, they are detected at about 8:00 UTC. For SCs, the peak value follows the same seasonal trend, but the highest values occur approximatively three hours before that of columnar contents. The peaks in SCs, associated with increases in traffic, agree with founding by Kendrick et al. (2015). The described features are visible in both workdays and weekends LUTs, although during workdays the absolute concentrations are higher. The minimum values recorded in August have no physical-chemical motivation as they are related to lower vehicular flows due to holidays.

The observed diurnal and seasonal variations agree with results by Voiculescu et al. (2020), who analyzed NO2 atmospheric content measured by a traffic station in Braila, a Romanian city. They observed two diurnal peaks of the NO2 surface concentration at 07:00 UTC and 18:00 UTC, more evident during wintertime, associated with peaks in vehicular traffic. In the present study, the morning peak at 8:00 UTC is well evident both in the urban and semi-rural sites while the evening peak is not detectable. The same diurnal behavior has been identified in Rome by Bassani et al. (2021), analyzing the urban and rural traffic stations belonging to the Regional Agency for Environmental Protection (ARPA Lazio, http://www.arpalazio.gov.it/ambiente/aria/). They found that the NO2 reached a morning peak between 07:00 and 09:00 UTC, and a second peak between 20:00 and 22:00 UTC, higher than the morning one. Unfortunately, Pandora measurements end just before the sunset: during summer, they stop at about 18:00 UTC while, in the winter months, due to the shorter duration of daytime hours, the measurements typically end at 15:00 or 16:00 UTC. Nonetheless, a slight increase in NO2 SC in the evening hours during the warm months is still noticeable, more evident in the APL urban site, both for workdays and for weekends. Moreover, the seasonal variation of NO2 SC agrees with founding by Voiculescu et al. (2020), even if it is less marked. In Rome, during the winter, NO2 SC remains quite high throughout the day (values between 8 and 14 ppb for APL and between 5 and 12 ppb for CNR-ISAC), assuming higher values only at the morning peak (10 to 14 ppb for both sites). On the contrary, during spring and, above all, summer, despite the morning highest values due to vehicular traffic (up to 18 ppb for both sites), the monthly average is lower (about 5 ppb for both APL and CNR-ISAC). The winter increase is linked to several concomitant factors. First, in winter the uniform, daily concentration is due to the increase in anthropogenic emissions because of domestic heating and to the slower photochemical reactions of NO2 (Anand and Monks, 2017; Beirle et al., 2003). Furthermore, the conditions of atmospheric stability and the possible presence of a thermal inversion layer are responsible for reduced vertical mixing that inhibits the dispersion of contaminants (Cattani et al., 2010). Finally, the atmospheric boundary layer height, significantly lower in winter, influences the wind pattern limiting the dilution of pollutants in a smaller volume of atmosphere and, consequently, exacerbating their accumulation close to the ground (Pichelli et al., 2014; Gariazzo et al., 2007).

Nevertheless, the summer reduction of the concentration is not marked as in Voiculescu et al. (2020). This difference is attributable to the different extents of the cities analyzed.

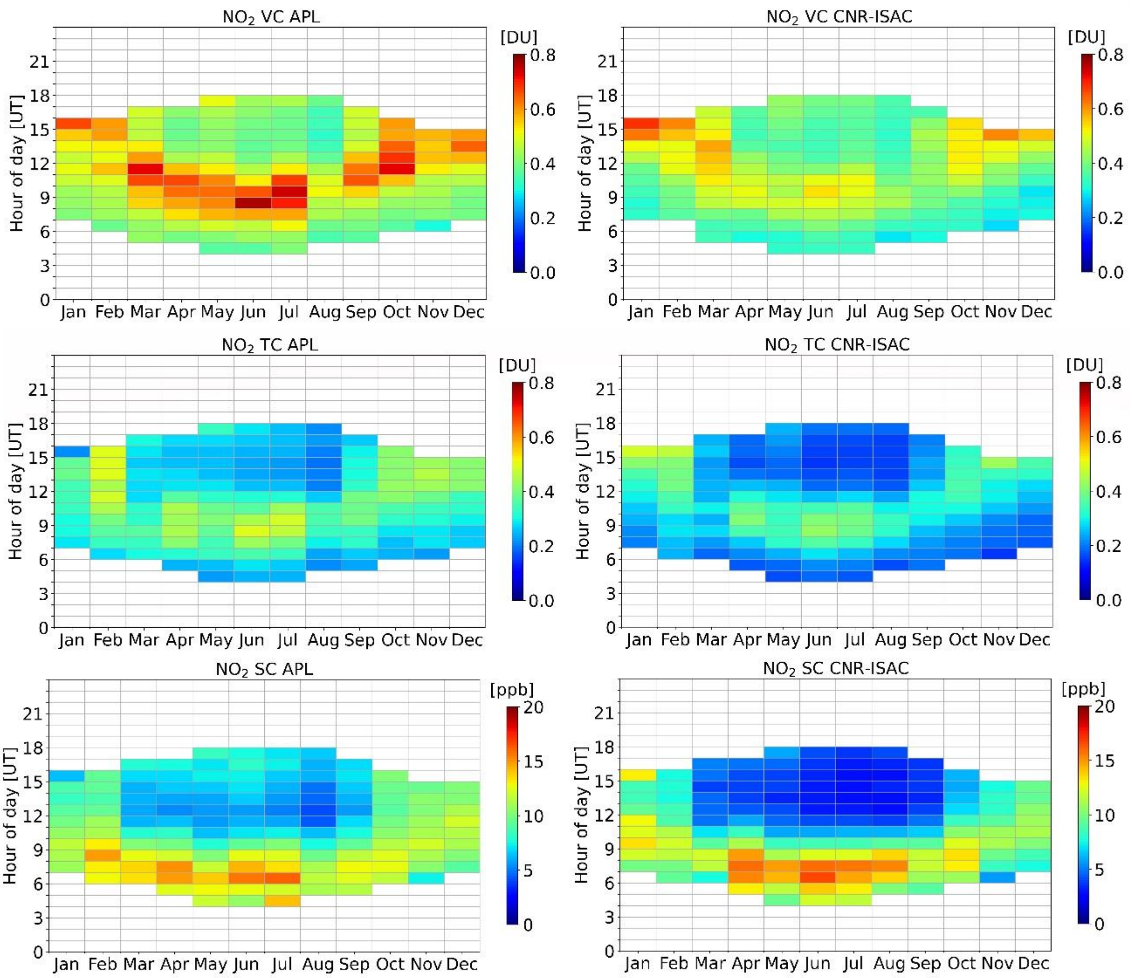

Braila, in fact, is a small urban center with a population equal to 8% of that of Rome and an extension of about 2.5%. The anthropogenic sources and the pollutants background of the two cities are therefore not strictly comparable.

Figure 2: PGN NO_2 reference LUTs for workdays. Upper panels: VC, central panels: TC, lower panels: SC. Left column: APL, right column: CNR-ISAC.

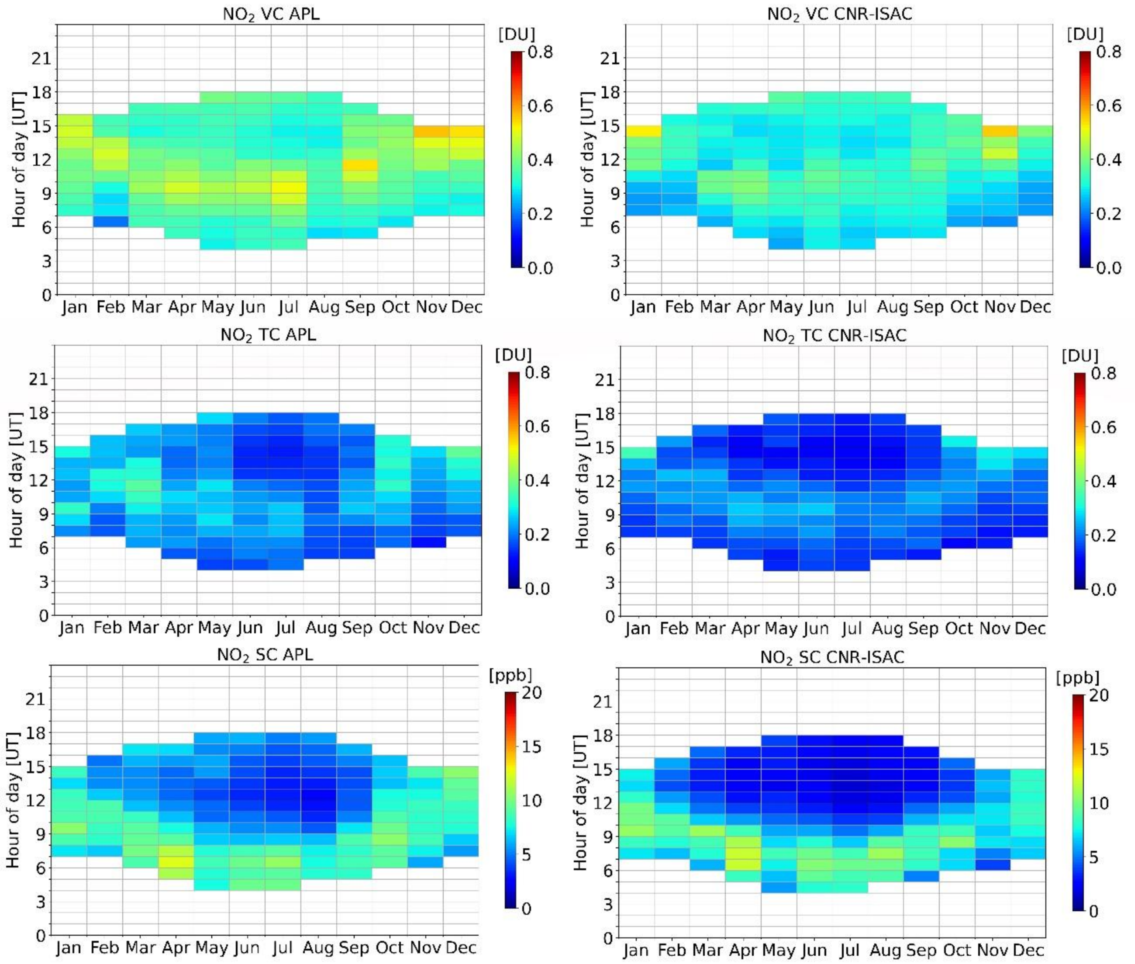

Figure 3: PGN NO_2 reference LUTs for weekends. Upper panels: VC, central panels: TC, lower panels: SC. Left column: APL, right column: CNR-ISAC.

4- THE LOCKDOWN PERIOD

In this Section the analysis is focused on the lockdown period, aiming to assess the impact of traffic restrictions on NO_2 concentrations.

As it is well known, the presence of NO_2 in an urban environment is mainly linked to emissions from local, vehicular sources. Therefore, a rigorous analysis of the factors influencing the NO_2 loads observed at the APL and CNR-ISAC sites must take into consideration the variations of the vehicular traffic and meteorological conditions occurred in the Rome area during the lockdown.

During 2020, various international organizations produced detailed information about the vehicle mobility variations in urban and rural areas around the world, now available to citizens and scientific community. For instance, Apple (https://covid19.apple.com/mobility, last accessed 9 September 2021), monitored private mobility in the Rome area. The analysis was carried out by considering the digital traces produced by navigation systems, maps, and mobile applications of Apple users. These data consist in the percentage difference of total mobility flows with respect to the period immediately preceding the lockdown (from 13 January to 16 February 2020). Data have been collected and aggregated over the whole area comprised in the Municipality of Rome. Therefore, these data provide general information about the total number of vehicles circulating in Rome, with no indications to their territorial distribution. The Apple dataset shows a pronounced mobility reduction (especially after the publication of DPCM-2), highlighting the huge impact of lockdown measures on traffic flows. In detail, traffic reduction starts with the publication of DPCM-1, reaching about -35% on 4 March, i.e., on the publication date of DPCM-2. After the publication of DPCM-2, the private mobility drops to over -80% during workdays and -90% during weekends. The traffic increases again during May, i.e., after the reopening of some factories and activities on 4 May (-60%), and June (-40%), reaching about pre-lockdown levels during July.

Moreover, Google LLC developed the project “Google COVID-19 Community Mobility Reports” (https://www.google.com/covid19/mobility/, last accessed 9 September 2021), in which the variations in movement are tracked over time by geography, across different categories of places such as retail and recreation, groceries and pharmacies, parks, transit stations, workplaces, and residential areas. In this dataset, data are compared with a reference value computed as the median value, for the corresponding day of the week, during the 5-week period from January 3 to February 6, 2020. During the lockdown period, the results show a decrease in mobility in the considered categories, except for residences, where mobility increased (about 25%). In particular, the decrease is more pronounced in recreational areas and in public transport (about 70%). From the month of May, a slight increase in mobility is recorded, due to the resumption of many activities.

Unfortunately, all these data are provided only for the lockdown period or, at most, from spring 2020 onwards. This implies that no solid conclusion can be drawn about long term trends. Furthermore, the data have a heterogeneous spatial and temporal resolution and are aggregated following different criteria, not allowing quantitative analyses. Nevertheless, all datasets show a net reduction of vehicular traffic and, consequently, of local NO_2 emissions during spring 2020.

In order to qualitatively evaluate the possible impact of the atmospheric circulation on the NO_2 values observed during the examined period, the hourly wind intensity measured by a ground-based meteorological station (Campbell Scientific Ltd Loughborough, United Kingdom) was further considered. The station belongs to the Regional Agency for the Development and Innovation of Agriculture of Lazio (ARSIAL, http://www.arsial.it/arsial/) and it is located in the urban center of Rome at about 2 km from the APL site (41.921 N, 12.523 E, 36 m.a.s.l.).

The wind data of 2020 are compared with those collected from 1st January 2016 to 31st December 2019. A LUT has been calculated using the same criteria described in the previous Section but without differentiation between workdays and weekends. The resulting interpolated reference daily cycles (IRDCs, see Section 3.1 for details about the definition) have been compared with the daily averaged wind intensity collected during lockdown. Figure 4 shows the daily averages of wind intensity with their standard deviation (error bars); the blue line indicates the wind IRDC means while the shaded area the one standard deviation statistical variation.

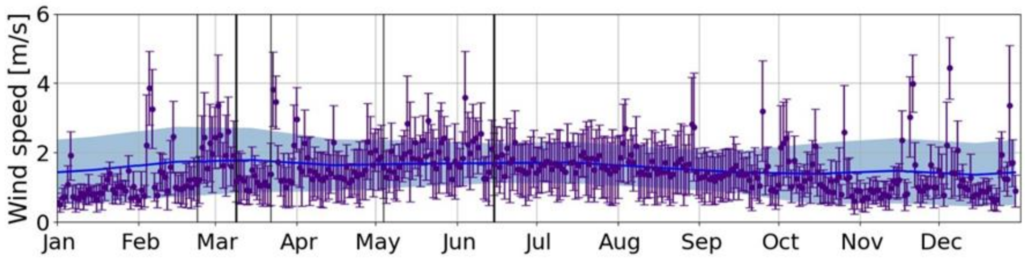

Figure 4: Daily averages of wind intensity measured by ARSIAL meteorological station during 2020 with standard deviation (error bar) compared with IRDC values with their one standard deviation (blue line and shaded area). The vertical lines display the publication dates of the DPCMs 1, 2 and 3, the 4 May 2020 and the official end of lockdown period (DPCM-2 and the end of lockdown are marked by thicker lines).

The large part of the lockdown period is characterized by wind intensity typically below the IRDC means, although in the statistical variability range. Nonetheless, some periods characterized by relatively stronger winds (>2 m/s) are observable during the lockdown: between DPCM-1 and DPCM-2, in the middle ten days of May and in the first week of June. Spring windy days are due to highly energetic phenomena, which, in the recent years, take place more and more frequently in the central region of the Mediterranean Sea (Michaelides et al., 2018) and are dominated by mesoscale weather conditions (Di Bernardino et al., 2021). Furthermore, lower rainfall (17.2 mm of accumulated rainfalls) and higher temperatures (15 °C) with respect to the monthly average of the period 1971-2001 (57.8 mm and 10.2 °C, respectively) characterized March 2020 (http://clima.meteoam.it/AtlanteClimatico/). This suggests that the dispersion of pollutants into the atmosphere has been poorly affected by the washout effect due to the rain and by the mechanical dispersion due to the wind.

Analysis of NO2 concentrations by Pandora

The approach to assess the differences between the reference and the investigated NO_2 products is designed as follows:

(i) for each day, the NO_2 VC, TC and SC data are quality screened as described in previous Sections;
(ii) the analyzed day is classified as workday or weekend, with the association of the corresponding LUT;
(iii) the chosen LUT columns, representing the monthly means values at different hours, are linearly interpolated to the selected day, to produce a reference daily cycle (RDC, in which each column is associated with the 15th day of the respective month);
(iv) the RDC is interpolated to the times in which measurements of the selected day have been performed (IRDC);
(v) the IRDC values are compared to the corresponding retrievals in terms of daily mean of IRDC and actual retrievals, daily standard deviations of IRDC and actual retrievals, daily mean absolute difference, daily mean percentage difference and standard deviation of daily differences. The retrievals were screened following the same criteria described in

the LUTs construction (DQF=0, 1, 10, 11, maximum solar zenith angle 80 degrees, maximum relative retrieval uncertainty 10% for VC and 40% for TC and SC).

The rationale for designing this approach is that the daily coverage of PGN products is usually not uniform, especially for direct Sun measurements, e.g., due to the presence of clouds in the field of view affecting the data quality. In general, only a portion of the NO_2 daily cycle can be covered in a single day with good quality data. Consequently, this incomplete sampling could significantly influence the deviations with respect to the reference, if not accounted for. As an example, Figure 5 shows the Pandora APL measurements (red dots) of 17 April 2019 and 26 April 2019 compared to the RDC mean values and standard deviation (blue line and shaded area, respectively). During the first day, the entire RDC values will be used to calculate the daily reference value while, during the second day, the daily average of measurements will be compared with just the first and the last part of the RDC. Furthermore, the use of workday and weekend LUTs assures to avoid oscillation in the difference between the daily means of actual retrievals and IRCD caused by the reduced values of NO_2 during weekends.

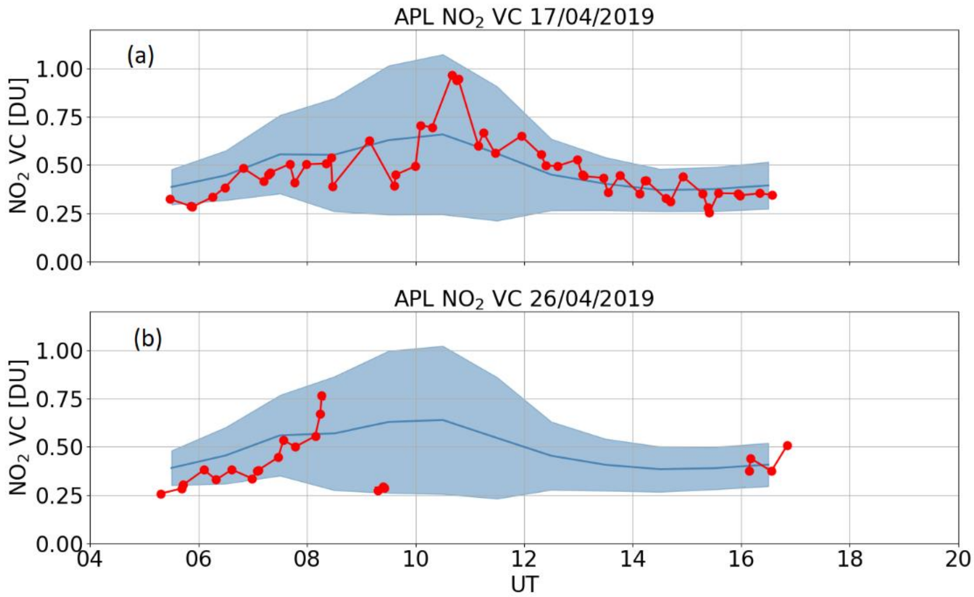

Figure 5: (a) 17 April 2019 and (b) 26 April 2019NO_2VC data collected by Pan#117 (red dots) compared with the RDC mean values (blue line) and standard deviation (shaded area).

Figures 6 and 7 show the time series of the daily average values retrieved by BAQUNIN Pandora instruments during 2020 and their relative differences with respect to the reference dataset, for NO_2 TC. The same graphs were also produced for NO_2 VC and SC but, due to lack of space, they are not shown. In each Figure, the upper panel shows the daily averaged IRDC (blue line) and the daily averaged retrievals for both APL and CNR-ISAC (red dots). The shaded area shows the one standard deviation IRDC variability, while the red vertical bars indicate the quadratic sum of the standard deviation of the daily retrievals and the daily mean of the fitting uncertainties. The lower panel shows the evolution of percentage difference between lockdown data and reference dataset. The black vertical lines display (from left to right, respectively) the publication dates of the DPCMs 1, 2 and 3, the 4 May and the date of the official end of the Italian lockdown (15 June). The periodical oscillations of the IRDC means are due to the use of different LUTs for workdays and weekends.

The NO_2 TC values show a strong reduction after the publication of the DPCM-1, with relative difference with respect of the IRDC means over -75% for TC and SC measured at both APL and CNR-ISAC and over -60% and -75% for VC measured at APL and CNR-ISAC, respectively.

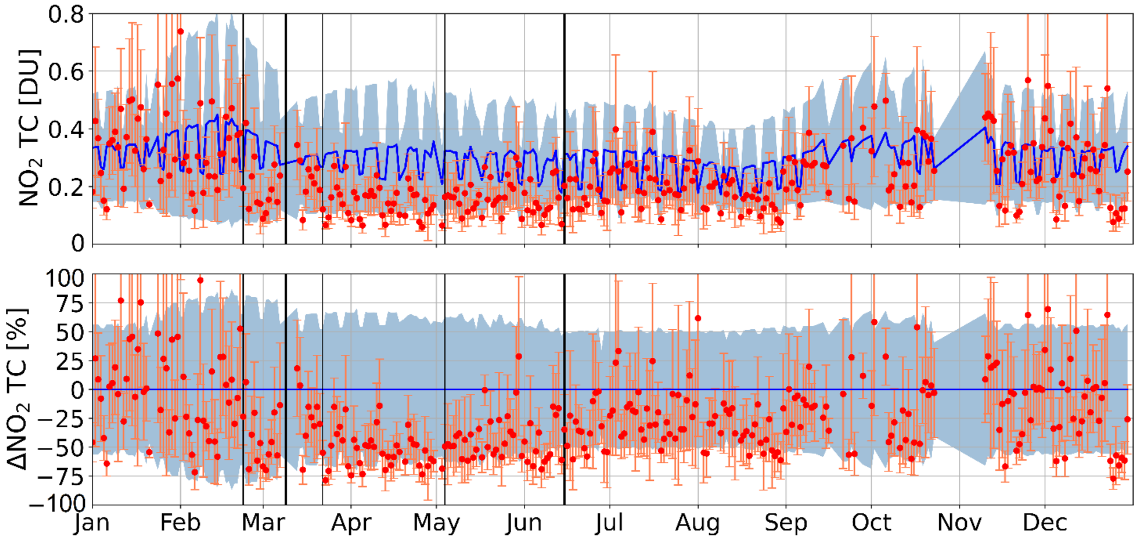

Figure 6: Time series (starting from January 1st, 2020) of the APL NO2 TC daily values for the lockdown period (upper panel) and the relative differences with respect the reference of NO_2 TC (lower panel). The vertical lines display the publication dates of the DPCMs 1, 2 and 3, the 4 May 2020 and the official end of lockdown period (DPCM-2 and the end of lockdown are marked by thicker lines), while the shaded area the IRCD one standard deviation.

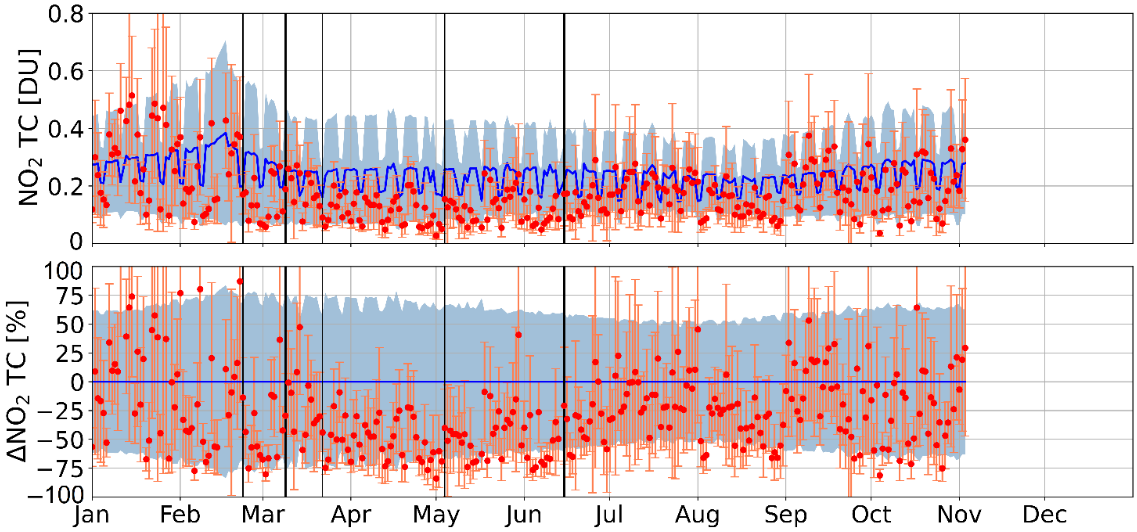

Figure 7: Time series (starting from January 1s, 2020) of the CNR-ISAC NO2 TC daily values for the lockdown period (upper panel) and the relative differences with respect the reference of NO2 TC (lower panel). The vertical lines display the publication dates of the DPCMs 1, 2 and 3, the 4 May 2020 and the official end of lockdown period (DPCM-2 and the end of lockdown are marked by thicker lines), while the shaded area the IRCD one standard deviation.

Table 2 summarized the mean values and standard deviations of retrievals and the relative differences with respect to the IRDC means obtained during the lockdown. The differences calculated for TC and SC are comparable with the results obtained in other studies analyzing air quality of large urban areas during lockdown measures through air quality stations and satellite data. Baldasano (2020) found a reduction of NO_2 concentration during the Spanish lockdown of 50% for Barcelona and 62% for Madrid with respect to the month of March 2019. Also, Tobias et al. (2020) investigated the changes in air pollution levels during the lockdown in the city of Barcelona by analyzing the time evolution of black carbon, NO_2, O_3 and particulate matter recorded by ground-based air quality stations. They estimated a strong reduction (about 50%) for NO_2 atmospheric concentration. Moreover, Siddiqi et al. (2020) studied NO_2 concentrations for eight major Indian cities, focusing on the air quality levels before and during the lockdown through satellite and ground-based measurements. Their results showed a mean reduction of NO_2 concentration of about 46%. Nevertheless, it is important to underline that all these studies compare the amount of NO_2 during the lockdown with the immediately preceding period or, at most, with the same month of the previous year, and not with a statistic calculated on multi-year data series.

	NO_2 TC[DU]	ΔNO_2 TC [%]	NO_2 VC [DU]	ΔNO_2 VC [%]	NO_2SC [ppb]	ΔNO_2 SC [%]
APL	0.16 (0.06)	45 (20)	0.29 (0.06)	37 (13)	5.2 (2.5)	37 (27)
CNR-ISAC	0.13 (0.06)	49 (20)	0.24 (0.06)	38 (13)	5.1 (2.5)	29 (29)

Table 2: Mean values and differences with standard deviation of the NO_2 during the period 9 March – 15 June 2020.

Figure 8 shows the monthly average concentration of NO_2 expressed as deviation with respect to the IRDC calculated for TC, VC and SC respectively, with their standard deviations (shaded area). April is the month characterized by the minimum NO_2 concentration for both APL and CNR-ISAC (ΔNO_2 VC=43% and 42%, ΔNO_2 TC=54% and 50%, ΔNO_2 SC=45% and 34% for APL and CNR-ISAC, respectively). TC and VC measured at both APL and CNR-ISAC and SC measured at APL slowly increased after the end of the lockdown, although with concentrations lower than the IRDC. CNR-ISAC SC measurements reveal a slight increase of NO_2 during summer with respect to the reference data, reaching its maximum in September (increase of about 50%). However, CNR-ISAC SC measurements from July onwards are characterized by the degradation of the instrument tracker that involves a worsening in the inversion of the data. Hence, a degree of caution should be exercised in the interpretation of these high values.

Although mobility and wind intensity data provide just a qualitative scenario of the lockdown period, their analysis corroborates the interpretation of the NO_2 trends. From the anemological point of view, three peculiar periods can be detected. From 22 February to 9 March, traffic has a decrease of about 25% while meteorological conditions are characterized by stronger winds with respect to the reference IRDC means. The combination of these two factors could explain the relative minima NO_2 concentrations measured both at APL and at CNR-ISAC. According to the mobility data between 22 March and 4 May, the values of vehicles circulation were lowest (traffic reduction was of the order of 75%, with minima of 90% or less), in the absence of sustained strong winds. However, while April is indeed characterized by the lowest NO_2 levels, differences with respect to the preceding month appear to be constrained by the decrease in wind-induced dispersion. The third period starts from 4 May, when the vehicles mobility slowly increases, with oscillations in the NO_2 concentration values that could be related to the meteorological conditions (alternation of periods of stronger and weaker wind intensity) during the mid of May and first part of June.

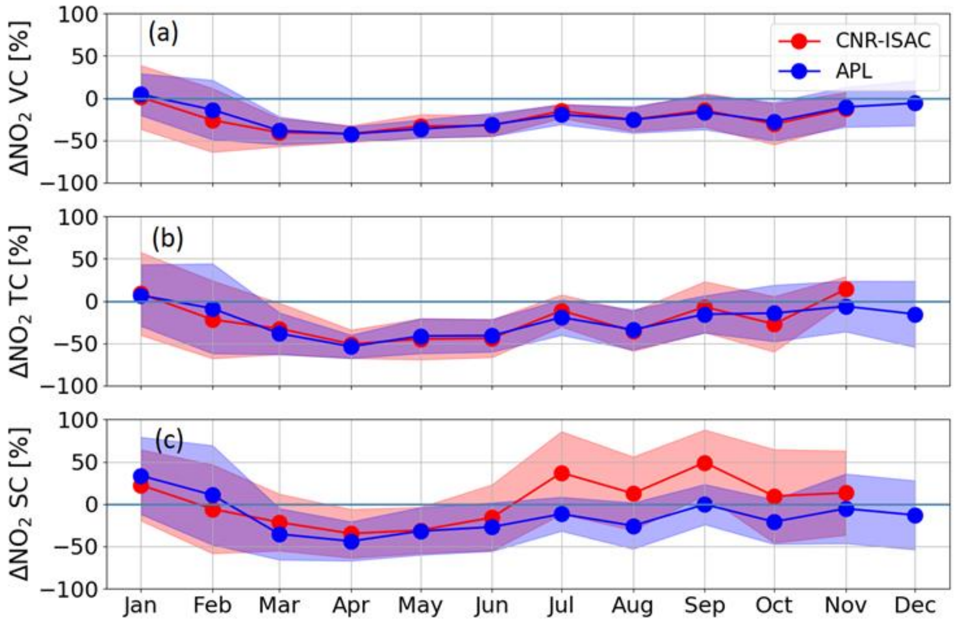

Figure 8: Monthly averages of NO_2 VC (a), TC (b) and SC (c) deviation with respect to the IRDC with their standard deviations (shaded area). Blue line refers to APL, red line to CNR-ISAC.

Comparison of NO2 surface concentrations retrieved by Pandora and by urban air quality stations

In this Section, the comparison between the differences of surface concentrations of NO_2 with the reference dataset as retrieved by Pandora and by the ground-based stations belonging to the air quality monitoring network managed by Regional Environmental Protection Agency of Lazio region (ARPA Lazio, http://www.arpalazio.gov.it/ambiente/aria/) is carried out. ARPA reference has been calculated using data from 1 January 2017 to 31 December 2019.

As shown in Table 3, only the stations located within a radius of 8 km from the APL and CNR-ISAC measurement sites were considered. Hourly-averaged NO_2 concentrations were sampled by each station using a Teledyne-API 200E analyzer (Teledyne Instruments, San Diego, California, U.S.A.) and have been collected to obtain weekly-averaged values. The air quality stations are classified as "urban traffic" if located on sidewalk of highly trafficked streets and "urban background" if installed near secondary roads or on the edge of urban green areas. The NO_2 values obtained by the six stations considered for APL and by the two stations close to ISA-CNR (see Table 3) were averaged to provide a temporal trend for the year 2020 comparable with the Pandora data. Since the air-quality stations retrieve the NO_2 concentration in µg/m^3, while Pandoras provide NO_2 SC in ppb, in what follows the relative differences of weekly-averaged concentrations with respect to the relative reference dataset are shown.

Figure 9 depicts the temporal trend of the NO_2 in situ (surface) concentration deviations from reference as estimated from ARPA data, superimposed to the NO_2 SC obtained from the Pandora during 2020 for APL (panel a) and CNR-ISAC (panel b). Although the ARPA data are derived from stations located in different locations of the city (although close to the APL and CNR-ISAC sites) and the Pandora measurements are carried out at the roof of a six-story building and not at street level, the NO_2 variation trends show a very satisfactory agreement.

Station	Latitude	Longitude	Altitude (m.a.s.l.)	Distance from measurement site (km)	Environment
Magna Grecia	41.883	12.509	49	2.15 (APL)	Urban traffic
Preneste	41.886	12.541	37	2.75 (APL)	Urban background
Tiburtina	41.910	12.549	32	2.90 (APL)	Urban traffic
Arenula	41.894	12.475	31	3.45 (APL)	Urban background
Villa Ada	41.933	12.507	50	3.54 (APL)	Urban background
Bufalotta	41.948	12.533	41	5.32 (APL)	Urban background
Fermi	41.864	12.469	26	5.66 (APL)	Urban traffic
Cipro	41.906	12.447	31	5.66 (APL)	Urban background
Francia	41.947	12.469	43	6.36 (APL)	Urban traffic
Cinecittà	41.858	12.569	53	6.56 (APL) 5.79 (CNR-ISAC)	Urban background
Ciampino	41.798	12.607	134	6.92 (CNR-ISAC)	Urban traffic

Table 3: information on the air quality stations managed by ARPA Lazio. The measurement site for which the station was considered is indicated in brackets.

It can be noted that, after the emanation of DPCM-1, the NO_2 SC decreases considerably in both APL and CNR-ISAC sites according to the sharp reduction in traffic flow. At APL, the recorded reductions are about 55% (PGN) and 25% (ARPA) while, in the semi-rural site of CNR-ISAC, the Pandora marks a decrease of about 60% and ARPA of approximatively 40%. Immediately after the entry into force of the DPCM-1, the concentration variations measured by PGN and ARPA instruments are very similar. During the lockdown, the two networks detect significant reductions in NO_2 SC: ARPA records reductions up to 65%, while PGN up to 60%. The decrease in the ARPA's data is comparable in both urban and the semi-rural sites. After the end of the lockdown, the SCs tend to recover to "normal situation" but, for the whole 2020, the average concentrations remain well below the ones computed using the reference dataset. In fact, according to ARPA, the decrease is about 25% in the urban area and 30% in the semi-rural area. The urban Pandora data are slightly more fluctuating than those collected by ARPA and, after the lockdown, show an average reduction of approximately 13%. In the CNR-ISAC site, the evaluation is made more difficult by the increase of variability in SC data from July onwards. As said, this is due to a progressive degradation of the performances of the instrument pointing accuracy, resulting in an increase of the noise level in the SC products. Therefore, CNR-ISAC results after July must be considered with caution.

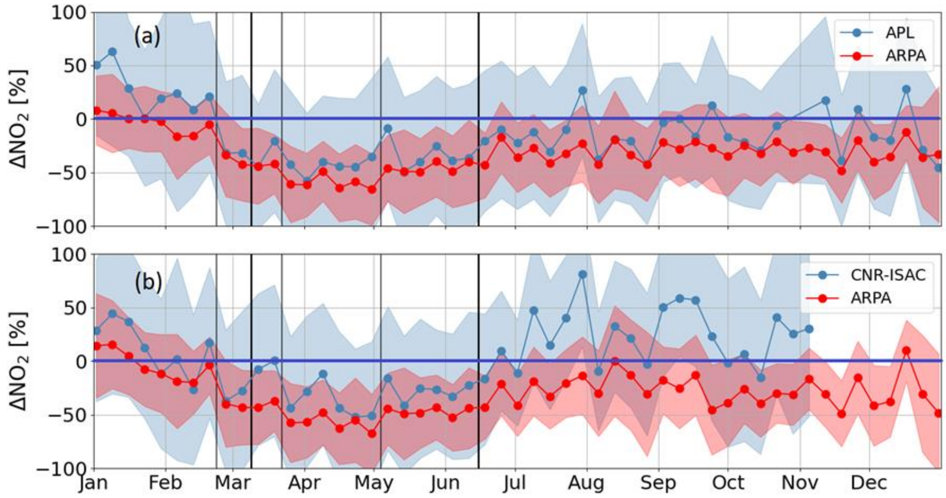

Figure 9: Relative differences of weekly-averaged NO_2 SC collected by Pandora and by ARPA air quality stations during 2020 with respect the reference of NO_2 SC at APL (a) and CNR-ISAC (b). The vertical lines display the publication dates of the DPCMs 1, 2 and 3, the 4 May 2020 and the official end of lockdown period (DPCM-2 and the end of lockdown are marked by thicker lines), while the shaded areas represent the data 1σ variability.

Even if the Pandora and ARPA measurements have been collected by means of tools and analysis methodologies completely different, the trends show very good agreement. This demonstrates the robustness of the Pandora data inversion algorithm and allows the analysis to be extended also to the total and tropospheric columnar content of NO_2.

Albeit preliminary and mainly based on qualitative considerations, these results confirm the impact of traffic volumes in determining NO_2 concentrations as measured via remote sensing techniques. They also indicate that a rigorous analysis of the driving processes, and therefore their effective monitoring, cannot prescind from detailed information on the traffic flows, on the local boundary layer stability, and on the synoptic meteorological conditions. The coordinated use of multiple remote sensing instruments, spatially distributed over the area of interest and coupled to traditional meteorological stations, can be expected to provide the necessary deeper insight, also in support to successful mitigation planning.

TROPOMI vs BAQUNIN PANDORA NO2 VCD inter-comparison

The TROPOspheric Monitoring Instrument (TROPOMI) was launched on board of ESA's Sentinel-5 Precursor (S5P) early-afternoon LEO satellite in October 2017. This hyperspectral imaging spectrometer measures the Earth's radiance, at 0.2–0.4 nm resolution in the visible absorption band of NO2, over ground pixels as small as 7x3:5 or 5:5x3:5 km^2 (before and after the switch to smaller pixel size on 6 August 2019, respectively) and with an almost daily global coverage thanks to a swath width of 2600 km.

TROPOMI L2_NO2 nitrogen dioxide summed column data (troposphere + stratosphere) are routinely compared to reference measurements acquired by Pandora instruments. They perform network operation in the context of the Pandonia Global Network (PGN).

Constantly updated validation reports are also available, see e.g., "S5P Routine Operations Consolidated Validation Report April 2018 - September 2021" at https://mpc-vdaf.tropomi.eu/index.php/nitrogen-dioxide?start=3

The S5p and PGN data are time and space collocated by adopting the following approach (Verhoelst et al., 2021), we reproduce here part of the mentioned article:

"*Only S5P pixels with a qa_value of at least 0.75 are retained. The so-called summed product is used, i.e., the total column computed as the stratospheric plus the tropospheric column values. This summed column differs from the total column product. Only Pandonia measurements with the highest quality label (0 and 10) are used. The average column value within a 1-hour time interval, centred on the S5P overpass time, is used. As the NO/NO2 ratio varies only slowly around the afternoon solar local time of the TROPOMI overpass, this small temporal window ensures no model-based adjustment is required. A 30 min time interval was tested as well, but this did not change the results significantly. Moreover, only TROPOMI pixels containing the station were considered. Except at low Sun elevation, the footprint of these direct Sun measurements is much smaller than a TROPOMI pixel. Therefore, as is the case with MAX-DOAS, a significant horizontal smoothing difference error can be expected in the TROPOMI–Pandora comparison, especially in the case of tropospheric NO2 gradients and when tropospheric NO2 is the largest contributor to the total column*."

The collocated datasets for each validation site can be freely downloaded from this URL: https://mpc-vdaf-server.tropomi.eu/no2. In what follows, the collocated PGN and S5p OFFL datasets for "Sapienza" (APL) and "Isacrome" (CNR-ISAC), downloaded from the above-mentioned URL, are analysed.

Figure 10 shows the PGN (blue square) and TROPOMI (red circles) NO2 VCD time series. Upper panel refers to APL, lower panel to CNR-ISAC. It should be noted that the CNR-ISAC time series is time limited to October 2020 due to maintenance of PAN#115 instrument (again operation by November 2021).

As reported in the S5p-MPC validation reports, the NO2 VCDs from BAQUNIN Pandoras tend to generally overestimate the S5p counterpart, especially for the APL urban site case.

However, during the Italian lockdown period, between March and July 2020, the satellite and ground-based data tend to converge to similar values.

This observation suggests that, as the NO2 produced by vehicle exhaust confined in the lower portion of the urban boundary-layer is significantly reduced, the satellite data provide a more accurate evaluation of the overall NO2 field.

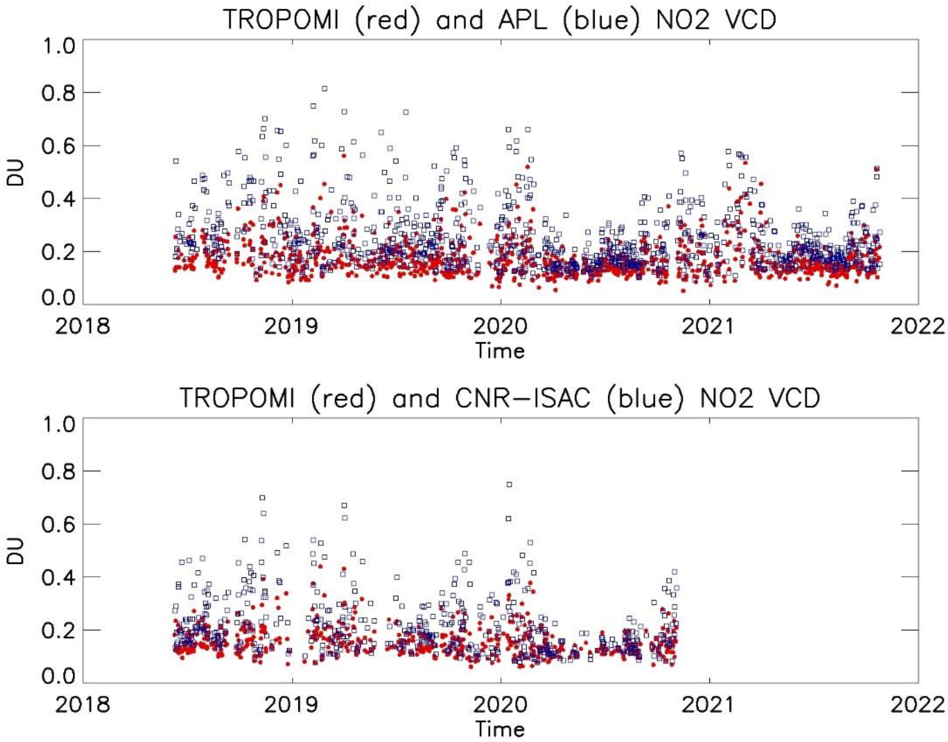

Figure 10: Time series of collocated TROPOMI and BAQUNIN Pandora NO2 VCD (DU). Upper panel: APL (Urban) site, lower panel: CNR-ISAC (semi-rural). Note that the CNR-ISAC time series is limited to October 2020 due to PAN#115 maintenance.

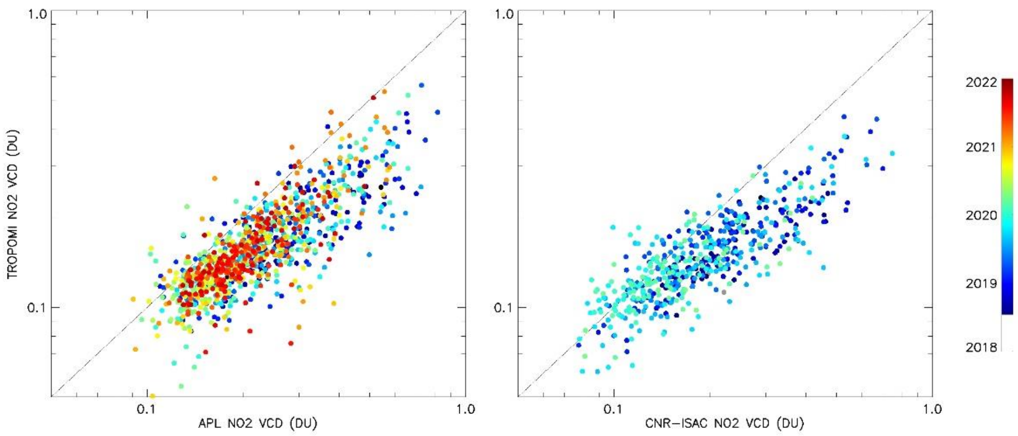

Figure 11: TROPOMI vs BAQUNIN Pandora NO2 VCD (DU). Left panel: APL (Urban), right panel: CNR-ISAC (Semi-rural). The colour scale indicates the measurement time for each matchup.

The correlation between TROPOMI and BAQUNIN PGN NO2 VCDs is reported in Figure 11, in which the left panel refers to APL, the right one to CNR-ISAC.

The colour scale indicates the measurement time for each matchup, helping to detect a gradual shift towards the 1to1 correlation from mission start onward.

The changes in the TROPOMI spatial resolution after August 2019 certainly reduce the so called "collocation error", but further analysis is needed to come to rigorous conclusions.

In order to quantify the possible differences between TOPOMI and BAQUNIN-PGN data, three periods have been analysed separately:

a) From June 2018 to July 2019: "undisturbed", TROPOMI resolution 7x3.5 km2
b) From August 2019 to February 2020: "undisturbed", TROPOMI resolution 5.5x3.5 km2
c) From March 2020 to September 2020: "lockdown", TROPOMI resolution 5.5x3.5 km2

The third temporal segment has been limited to September 2020 in order to account for PAN#115 unavailability after that date.

The S5p-PGN NO2 VCD statistics are computed for each selected period and for the two BAQUNIN sites separately, through the evaluation of the following parameters:

BIAS = average S5p-PGN absolute difference (DU)

RME = standard deviation of S5p-GND absolute difference (DU)

RMSE = standard deviation of S5p-PGN difference after removal of linear fit (DU)

CUNC = squared average of quadratic sum of S5p and PGN uncertainties (DU)

CORR = S5p vs PGN Pearson correlation coefficient

The statistical results are reported in Table 4.

Site	BIAS	RMS	RMSE	CUNC	CORR
From June 2018 to July 2019					
APL	-0.105	0.087	0.042	0.039	0.78
CNR-ISAC	-0.071	0.073	0.031	0.033	0.83
From August 2019 to February 2020					
APL	-0.093	0.080	0.042	0.053	0.85
CNR-ISAC	-0.073	0.081	0.036	0.043	0.82
From March 2020 to September 2020					
APL	-0.046	0.039	0.021	0.024	0.75
CNR-ISAC	-0.017	0.032	0.022	0.024	0.63

Table 4: S5p vs BAQUNIN PGN statistics

As expected, in the first two "undisturbed" periods PGN VCDs show a significant bias with respect S5p products, hence the bias seems to be not much affected by the increased spatial resolution of TROPOMI. However, during the "lockdown" period, the bias for the Urban site (APL) is -0.046 DU, with more than 50% reduction with respect the "undisturbed" periods. For the semi-rural site (CNR-ISAC), the bias almost vanishes during lockdown.

Same significant decrease is observed for the RMS, RMSE and CUNC parameters: this is a further indication that S5p sensitivity to high NO2 values is still not sufficient to detect extreme NO2 concentrations located in the lower portion of the atmospheric boundary layer.

It should be noted that RMSE and CONC values are very similar in all considered periods, thus indicating that the S5p and PGN reported (random) uncertainties are correctly estimated.

Finally, the correlation coefficient shows an increase after improvement of S5p spatial resolution, while decreases during the lockdown period. The latter consideration can be easily explained by the reduced range of observed NO_2 VCDs, which significantly impacts the estimate of correlation coefficients.

In conclusion to this paragraph, both TROPOMI and BAQUNIN PGN data observed a very well correlated significant reduction of NO_2 VCDs in correspondence of the Italian lockdown period, for both Urban (APL) and Semi-rural (CNR-ISAC) BAQUNIN sites. The most significant impact was, as expected, detected in correspondence of the urban site.

REFERENCES

Anand, J. S., Monks, P. S., 2017. Estimating daily surface NO2 concentrations from satellite data–a case study over Hong Kong using land use regression models. Atmos. Chem. Phys., 17(13), 8211-8230. DOI: 10.5194/acp-17-8211-2017.

Baldasano, J. M., 2020. COVID-19 lockdown effects on air quality by NO2 in the cities of Barcelona and Madrid (Spain). Sci. Total Environ., 741, 140353. DOI: 10.1016/j.scitotenv.2020.140353.

Beirle, S., Platt, U., Wenig, M., Wagner, T., 2003. Weekly cycle of NO2 by GOME measurements: a signature of anthropogenic sources. Atmos. Chem. Phys., 3(6), 2225-2232. DOI: 10.5194/acp-3-2225-2003.

Campanelli, M., Iannarelli, A. M., Mevi, G., Casadio, S., Diémoz, H., Finardi, S., Dinoi, A., Castelli, E., di Sarra, A., Di Bernardino, A., Casasanta, G., Bassani, C., Siani, A. M., Cacciani, M., Barnaba, F., Di Lioberto, L., Argentini, S., 2021. A wide-ranging investigation of the COVID-19 lockdown effects on the atmospheric composition in various Italian urban sites (AER–LOCUS). Urban Climate, *39*, 100954. DOI: .

Cattani, G., di Bucchianico, A. D. M., Dina, D., Inglessis, M., Notaro, C., Settimo, G., Viviano, G., Marconi, A., 2010. Evaluation of the temporal variation of air quality in Rome, Italy from 1999 to 2008. Ann. Ist. Super. Sanità, 46, 242-253.

Cede, A., 2019. Manual for Blick Software Suite Version 12, available on https://www.pandonia-global-network.org/wp-content/uploads/2019/11/BlickSoftwareSuite_Manual_v1-7.pdf.

Cede, A., Tiefengraber, M., Gebetsberger, M., and Kreuter, A., 2019. LuftBlick_FRM4AQ_PGNUserGuidelines_RP_2019009_v1, available on https://www.pandonia-global-network.org/wp-content/uploads/2020/01/LuftBlick_FRM4AQ_PGNUserGuidelines_RP_2019009_v1.pdf.

Di Bernardino, A., Iannarelli, A. M., Casadio, S., Mevi, G., Campanelli, M., Casasanta, G., Cede A., Tiefengraber M., Siani A.M., Spinei E., Cacciani M., 2021. On the effect of sea wi regime on aerosols and gases properties in the urban area of Rome, Italy. Urban Climate, 37, 100842. DOI: 10.1016/j.uclim.2021.100842.

DPCM-1: https://www.gazzettaufficiale.it/eli/id/2020/02/23/20A01228/sg.

DPCM-2: https://www.gazzettaufficiale.it/eli/id/2020/03/09/20A01558/sg.

DPCM-3: https://www.gazzettaufficiale.it/eli/id/2020/03/22/20A01807/sg.

DPCM-4: https://www.gazzettaufficiale.it/eli/id/2020/05/17/20A02717/sg.

DPCM-5: https://www.gazzettaufficiale.it/eli/id/2020/04/27/20A02352/sg.

ESA, 2020. Air pollution drops in India following lockdown. Retrieved May 4, 2020, from http://www.esa.int/Applications/Observing_the_Earth/Copernicus/Sentinel-5P/Air_pollution_drops_in_India_following_lockd.

Gariazzo, C., Silibello, C., Finardi, S., Radice, P., Piersanti, A., Calori, G., Cecinato, A., Perrino, C., Nussio, F., Cagnoli, M., Pelliccioni, A., Gobbi, G.P., Di Filippo, P., 2007. A gas/aerosol air pollutants study over the urban area of Rome using a comprehensive chemical transport model. Atmos. Environ., 41(34), 7286-7303. DOI: 10.1016/j.atmosenv.2007.05.018.

Goldberg, D. L., Anenberg, S. C., Griffin, D., McLinden, C. A., Lu, Z., Streets, D. G., 2020. Disentangling the impact of the COVID-19 lockdowns on urban NO2 from natural variability. Geophys. Res. Lett., 47(17). DOI: 10.1029/2020GL089269.

Hashim, B. M., Al-Naseri, S. K., Al-Maliki, A., Al-Ansari, N., 2020. Impact of COVID-19 lockdown on NO2, O3, PM2. 5 and PM10 concentrations and assessing air quality changes in Baghdad, Iraq. Sci. Total Environ., 754, 141978. DOI: 10.1016/j.scitotenv.2020.141978.

Herman, J., Cede, A., Spinei, E., Mount, G., Tzortziou, M., Abuhassan, N., 2009. NO2 column amounts from ground-based Pandora and MFDOAS spectrometers using the direct-sun DOAS technique: Intercomparisons and application to OMI validation. J. Geophys. Res., 114 (D13307), DOI: 10.1029/2009JD011848.

Hönninger, G., von Friedeburg, C., Platt, U., 2004. Multi axis differential optical absorption spectroscopy (MAX-DOAS). Atmos. Chem. Phys., 4, 231–254. DOI:10.5194/acp-4-231-2004.

Kendrick, C. M., Koonce, P., George, L. A., 2015. Diurnal and seasonal variations of NO, NO2 and PM2. 5 mass as a function of traffic volumes alongside an urban arterial. Atmos. Environ., 122, 133-141. DOI: 10.1016/j.atmosenv.2015.09.019.

Liu, F., Page, A., Strode, S. A., Yoshida, Y., Choi, S., Zheng, B., Lamsal, L. N., Li, C., Krotkov, N. A., Eskes, H., van Der, A. R., Veefkind, P., Levelt, P. F., Hauser, O. P., Joiner, J., 2020. Abrupt declines in tropospheric nitrogen dioxide over China after the outbreak of COVID-19. Sci. Adv., 6(28). DOI:10.1126/sciadv.abc2992.

Mesas-Carrascosa, F. J., Pérez Porras, F., Triviño-Tarradas, P., García-Ferrer, A., Meroño-Larriva, J. E., 2020. Effect of lockdown measures on atmospheric nitrogen dioxide during SARS-CoV-2 in Spain. Remote Sens., 12(14), 2210. DOI: 10.3390/rs12142210.

Michaelides, S., Karacostas, T., Sánchez, J. L., Retalis, A., Pytharoulis, I., Homar, V., Romero, R., Zanis, P., Giannakopoulos, C., Bühl, J., Ansmann, A., Merino, A., Melcón, P., Lagouvardos, K., Kotroni, V., Bruggeman, A., López-Moreno, J.I., Berthet, C., Katragkou, E., Tymvios, F., Hadjimitsis, D.G., Mamouri, R.-E., Nisantzi, A., 2018. Reviews and perspectives of high impact atmospheric processes in the Mediterranean. Atmos. Res., 208, 4-44. DOI: 10.1016/j.atmosres.2017.11.022.

Nakada, L. Y. K., Urban, R. C., 2020. COVID-19 pandemic: Impacts on the air quality during the partial lockdown in São Paulo state, Brazil. Sci. Total Environ., 139087. DOI: 10.1016/j.scitotenv.2020.139087.

Pichelli, E., Ferretti, R., Cacciani, M., Siani, A. M., Ciardini, V., Di Iorio, T., 2014. The role of urban boundary layer investigated with high-resolution models and ground-based observations in Rome area: a step towards understanding parameterization potentialities. Atmos. Meas. Tech., 7(1), 315-332. DOI: 10.5194/amt-7-315-2014.

Spinei, E., Tiefengraber, M., Müller, M., Cede, A., Berkhout, S., Dong, Y., and Nowak, N., 2020. Simple retrieval of atmospheric trace gas vertical concentration profiles from multi-axis DOAS observations, in preparation.

Verhoelst, T., Compernolle, S., Pinardi, G., Lambert, J.-C., Eskes, H. J., Eichmann, K.-U., Fjæraa, A. M., Granville, J., Niemeijer, S., Cede, A., Tiefengraber, M., Hendrick, F., Pazmiño, A., Bais, A., Bazureau, A., Boersma, K. F., Bognar, K., Dehn, A., Donner, S., Elokhov, A., Gebetsberger, M., Goutail, F., Grutter de la Mora, M., Gruzdev, A., Gratsea, M., Hansen, G. H., Irie, H., Jepsen, N., Kanaya, Y., Karagkiozidis, D., Kivi, R., Kreher, K., Levelt, P. F., Liu, C., Müller, M., Navarro Comas, M., Piters, A. J. M., Pommereau, J.-P., Portafaix, T., Prados-Roman, C., Puentedura, O., Querel, R., Remmers, J., Richter, A., Rimmer, J., Rivera Cárdenas, C., Saavedra de Miguel, L., Sinyakov, V. P., Stremme, W., Strong, K., Van Roozendael, M., Veefkind, J. P., Wagner, T., Wittrock, F., Yela González, M., and Zehner, C., 2021. Ground-based validation of the Copernicus Sentinel-5P TROPOMI NO_2 measurements with the NDACC ZSL-DOAS, MAX-DOAS and Pandonia global networks, Atmos. Meas. Tech., 14(1), 481–510. DOI: 10.5194/amt-14-615-2021.

WHO (World Health Organization), 2020. Coronavirus Disease 2019 (COVID-19) Situation Report January 12, 2020. World Health Organization Geneva. Available from: https://www.who.int/csr/don/12-january-2020-novel-coronavirus-china/en/ (accessed 2 January 2021).

WMO Guidelines on the Calculation of Climate Normals, 2017, WMO-No. 1203.

End of Document